Journal of Applied Physics PERSPECTIVE scitation.org/journal/jap

Engineering lattice metamaterials for extreme property, programmability, and multifunctionality

Cite as: J. Appl. Phys. **127**, 150901 (2020); doi: 10.1063/5.0004724
Submitted: 13 February 2020 · Accepted: 28 March 2020 ·
Published Online: 17 April 2020

Zian Jia,[1,2] Fan Liu,[1] Xihang Jiang,[1] and Lifeng Wang[1,a)]

AFFILIATIONS

[1]Department of Mechanical Engineering, State University of New York at Stony Brook, Stony Brook, New York 11794, USA
[2]Department of Mechanical Engineering, Virginia Polytechnic Institute and State University, 635 Prices Fork Road, Blacksburg, Virginia 24061, USA

[a)]**Author to whom correspondence should be addressed:** Lifeng.Wang@stonybrook.edu

ABSTRACT

Making materials lightweight while attaining a desirable combination of mechanical, thermal, and other physical properties is the "holy grail" of material science. Lattice materials, because of their porous structures and well-defined unit cell geometries, are suitable candidates to achieve lightweight with precisely tailored material properties. Aided by additive manufacturing techniques, a variety of lattice metamaterials with exceptional and unusual properties have been fabricated recently, yet, the rational designs of lattice metamaterials with programmability and multifunctionality are still challenging topics. In this perspective, we identify three emerging directions for lattice metamaterials: (1) developing architected lattice metamaterials with extreme and unusual properties that are non-typical in bulk materials, (2) designing lattice metamaterials with programmable mechanical properties that respond differently at different environments, loading paths, or controls, and (3) exploiting lattice metamaterials with multifunction, including tailorable thermal, mechanical, optical, piezoelectric, and negative-index material properties. These emergent directions portend the transitioning of lattice metamaterials from the stage of conventional materials to smart, adaptive, and versatile materials, which provide solutions to realistic problems in transport systems, wearable devices, and robotics, and continue to push the boundary of possibilities of architected metamaterials.

I. INTRODUCTION

Analogous to the lattice structure of a crystal, lattice materials typically refer to cellular materials with periodic arrangements of unit cells in two or three dimensions.[1] Among different material architectures, lattice structures can achieve the highest structure efficiency per unit weight;[2] therefore, they are broadly used in weight-critical applications like aerospace engineering, automobiles, armors, and rotor blades. Recently, the research interest in lattice metamaterials has expanded from purely mechanical to general physical, chemical, and biological properties. Figure 1 summarizes some characteristics of lattice metamaterials that are of particular interest in a wide range of scientific and engineering disciplines. New designs, functions, and applications are continuously and quickly added to this figure.

To illustrate the outstanding structural efficiency of lattice materials, let us review the history of developing lattice materials with ultra-high specific stiffness. About three decades ago, stochastic foams with cell sizes at the millimeter scale were developed and broadly used for thermal insulation and sandwich cores.[3,4] But the stiffness and strength of these stochastic foams degrade rapidly at low relative densities, flawed for lightweight applications. As such, designing materials that maximize stiffness and strength for a given density becomes an active research topic. Periodic micro-truss lattices were first proposed to tackle this problem, which was demonstrated to have a linear scaling relation between stiffness and relative density.[5] Such a linear scaling relation arises from a stretch-dominated deformation mechanism, which is later demonstrated to be common in truss lattices with high structural connectivity.[6] Later, the stiffest isotropic truss lattice was found by structural optimization.[7] However, the stiffest truss lattice achieves only ~30% of the Hashin–Shtrikman upper stiffness bound, suggesting that a different structure should be sought to reach the upper limit.

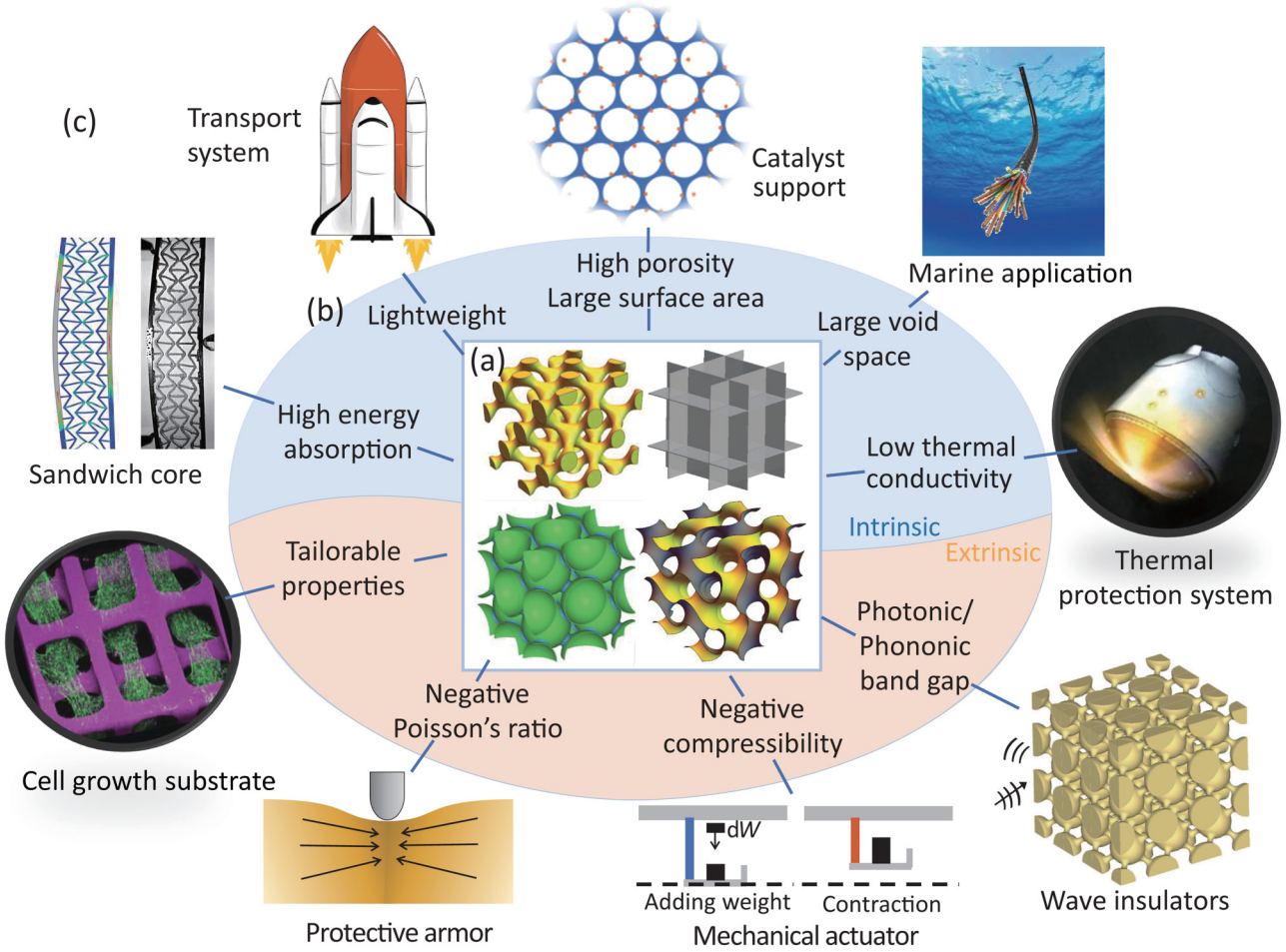

FIG. 1. Overview of lattice metamaterials: (a) structures, (b) properties, and (c) applications. The cell growth substrate panel is reproduced with permission from Kolewe *et al.*, Adv. Mater. **25**, 4459 (2013). Copyright 2013 Wiley.[48]

This upper limit has recently been achieved in plate-lattices.[8,9] The mechanism behind it is that plate connectivity presents stronger constraint than the truss connectivity, so substantially more strain energy can be stored in plate-lattices. With 3D printing, the proposed designs have been successfully fabricated, achieving a specific stiffness of 1.8×10^6 m^2/s^2 at a density of 14 mg/cm^3.[10,11]

The example above reveals the great potential of designing lattice materials to expand the material property space by spatial manipulation of the unit cell geometry. This is in stark contrast to traditional bulk materials, whose properties are dominated by the atomic structure which we still have limited control. Due to this constraint, traditionally, engineers have to select the "best material" from a given material library. This situation might change in the near future. As researchers are exploring artificial intelligence to design lattice materials,[12–14] we might be able to generate lattice material designs based on specific needs soon. Particularly, by exploiting the structure–property relationship of lattice materials, changes have taken place or are taking place in the following aspects: (1) precisely tailored material properties by precisely controlled lattice geometry, which includes not only stiffness and strength but also the entire stress–strain curve; (2) decoupling of material properties, which provides new avenues to break the material property trade-offs; and (3) arise of new physical properties, which gives rise to novel metamaterials.

Since many lattice metamaterials have complex 3D geometries, they pose significant challenges to traditional fabrication methods like perforated sheet folding/drawing,[15] wire/strip slot assembly,[16] and casting.[17] This manufacturing difficulty is overcome by advances in additive manufacturing. Currently, 3D printing offers precise control of the lattice geometry from the sub-μm to cm scale technology and it is evolving more rapidly than ever. Great advances have been made to improve print speed,[18–21] increase print precision,[22] and expand printable structures and materials.[21,23] Aided by these cutting-edge printing techniques, the study of lattice metamaterials

has achieved fruitful results. For instance, ultralight,[24] ultra-stiff,[11] and ultra-strong[25] lattices have been successfully fabricated. Besides, increasing research attention has been paid to the failure of lattice material, including plastic yield,[26–29] buckling,[30–33] fatigue,[34–36] and brittle fracture.[37–42] Recently, researchers start to treat these failure mechanisms differently—trying to take advantage of "failure" instead of avoiding them. For instance, buckling has been harnessed to produce metamaterials[43,44] and programmable materials.[45] Cracking has been controlled to improve toughness and is used as a manufacturing method.[46,47] Similar disruptive research is flourishing in the context of extreme materials and metamaterials, where more interesting designs and novel discoveries can be envisioned.

The study on lattice materials is broad and active—more than 50 000 papers are published in 2019. In this perspective, we will focus on three emerging directions, i.e., extreme lattice materials, programmable lattice materials, and multifunctional lattice materials. Most recent progress in these areas will be introduced and our related works will be presented. Useful design methodologies and promising structure features will also be discussed. Along the way, potential applications will be summarized, highlighting the challenges we are facing.

II. EMERGING DIRECTIONS

A. Extreme lattice metamaterials

Here, "extreme" is used to highlight lattice metamaterials whose properties are close to the theoretical limits or far beyond that of conventional bulk materials. Moreover, "extreme" also refers to the extreme control of a material's property (e.g., the whole stress–strain curve) by designing the unit cell. In the following, we will discuss four categories of extreme lattice metamaterials.

1. Ultra-stiff, strong, and tough lattice metamaterials

Materials are desired to have high stiffness (to resist deformation), high strength (to resists non-recoverable deformation), and high toughness (to absorb energy without fracturing). In order to achieve high specific stiffness at low density, linear scaling between stiffness and relative density is desired. Alongside the well-known octet lattices,[11] hollow sphere-binder assembles are also demonstrated to have a linear scaling relation,[44] as seen in Fig. 2(a). More recently, plate-lattices are shown by simulation to reach the theoretical upper bound stiffness of isotropic materials.[8,10] These results indicate that high structure constraint (plate connection provides a stronger constraint than truss connection) and even stress distribution are two critical conditions to achieve ultra-high stiffness. A stiffness comparison of the above three lattices with $E/E_s \propto \rho/\rho_s$ is shown in Fig. 2(a). The plate lattice possesses the highest stiffness, but high stiffness often means the lack of an easy deformation mode, thus typically leads to catastrophic fracture.[25,49] One way to prevent such catastrophic damage is by transferring the fracture-type failure to a buckling-type deformation using ultra-thin structures. Examples include thin-hollow ceramic lattices fabricated with a coating-etching approach, which recovery at a compressive strain of 50%.[50] More approaches to overcome the conflict between stiffness (strength) and toughness will be discussed in Sec. II A 2.

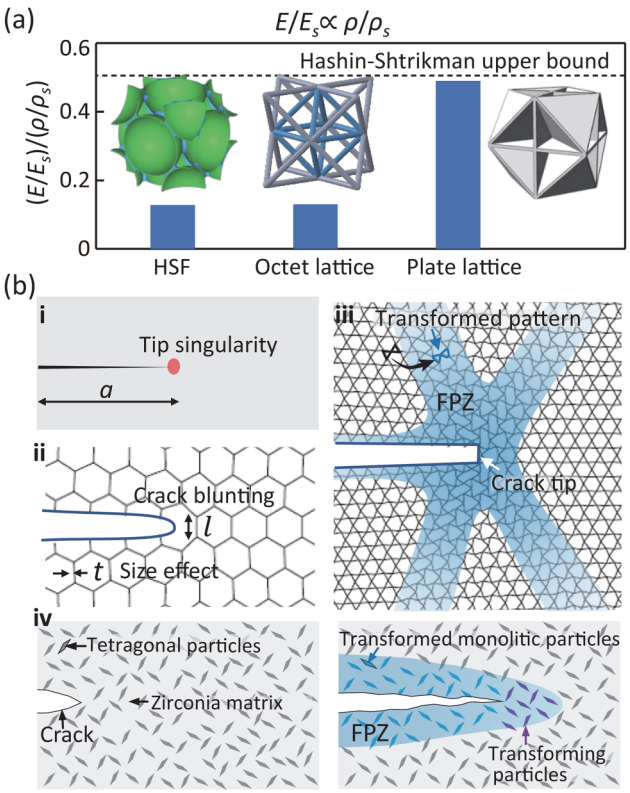

FIG. 2. Stiff, strong, and tough lattice metamaterials. (a) Lattice materials that possess linear scaling relations, $E/E_s \propto \rho/\rho_s$, the specific stiffness values are presented at $\rho/\rho_s = 0.03$. (b) Crack blunting effect in (ii) lattice materials compared to (i) tip singularity in bulk materials. (iii) Transformation-toughening (Kagome lattice) which is analogous to the transformation-toughening in (iv) zirconia. Lattice deformation image in (iii) is reproduced with permission from Fleck and Qiu, J. Mech. Phys. Solids **55**, 562 (2007). Copyright 2007 Elsevier.

Different from effective stiffness, the effective strength of a lattice material is determined not only by constituent material and topology but also by the structure size (thickness t). This is known as the size effect–a smaller structure tends to have less (and smaller) defects thus stronger ($\sigma_f \propto 1/\sqrt{t}$).[51,52] Exploiting this effect, theoretical material strength (defect-free materials possess $\sigma_f \sim E/10$) can be reached when the feature size (t) of a lattice material gets close to the fracture process zone size of the constituent material.[52,53] One estimation of this critical size is $t^* \sim \pi\gamma E/\sigma_{th}^2$, with γ, E, and σ_{th} being the surface energy, modulus, and theoretical strength, respectively.[53] For ceramics, the critical size is in the order $t^* \sim 100$ nm. As such, sub-micrometer size is required for a ceramic lattice to reach its theoretical material strength. Following this ideal, glassy carbon nanolattices with effective strengths of 1.2 GPa at 0.6 g cm^{-3} are fabricated by pyrolysis of polymeric microlattices with $t \sim 200$ nm.[25] Note that smaller is not always good, because the larger free surface of a smaller structure tends to reduce the barrier energy of deformation and make materials weaker.[54] It should also be highlighted that for lattice materials

with ultra-low density, buckling instead of cracking, could be the limiting factor of effective strength. Thus, improving the critical buckling load is also important to achieving the theoretical strength (hierarchy provides an efficient way to improve the critical buckling load[55]).

Compared to stiffness and strength, our knowledge of fracture toughness is much less complete. We know that in general, the fracture toughness of lattice materials (brittle fracture) satisfies the following scaling relation:[38,42]

$$K_{IC} = \alpha \bar{\rho}^{n} \sigma_{fs} \sqrt{l}, \tag{1}$$

where α and n are scale parameters, $\bar{\rho} = \rho/\rho_s$ is the relative density, σ_{fs} is the fracture strength of the solid, and l is the cell size [Fig. 2(b)]. For brittle constituent, $\sigma_{fs} = K^s_{IC}/\sqrt{2\pi a}$, determined by linear elastic fracture mechanics (LEFM), where a is the defect size. Note that truss thickness, t, provides a good presentation of the defect size a. Using Eq. (1), we then derive

$$\bar{K}_{IC} = \frac{K_{IC}/\rho}{K^s_{IC}/\rho_s} = \alpha' \bar{\rho}^{n-1} \sqrt{l/t}, \tag{2}$$

where $\bar{K}_{IC}$ is the normalized fracture toughness per weight and the superscript, s, refers to the solid constituent. For lattices with tensile controlled deformation (such as 2D triangular lattice and 3D octet lattice), $n \approx 1$.[40,42] As a result, $\bar{K}_{IC} \propto \sqrt{l/t}$ suggest that a larger cell size and a smaller truss thickness improve $\bar{K}_{IC}$. This result gives the rationale of designing lattice materials to achieve higher fracture toughness per weight than bulk materials. Specifically, the $\sqrt{l}$ term presents the crack blunting effect and the $\sqrt{t}$ term presents the defect tolerance at the truss thickness level [Fig. 2(b)]. Note that size l can be improved by introducing structural hierarchy. Because of these toughening mechanisms, crack insensitivity can be observed even in brittle lattice materials, e.g., lattice materials become strength controlled instead of linear elastic fracture mechanics (LEFM) controlled for cracks $<1.5l$–$4l$ depending on the lattice type.[42] This short crack tolerance is important to the design of robust (defect insensitive) brittle lattices.

To this point, fracture is assumed to take place at a single ligament in front of a crack tip. Some lattices may have a large fracture processing zone (FPZ) spanning multiple unit cells. One example is the Kagome lattice depicted in Fig. 2(b-iii), where several buckling bands radiate from the crack tip forming a large FPZ and significantly blunts the crack tip. Such a deformation morphology significantly improves the fracture toughness of the Kagome lattice, which has a scaling parameter, $n = 0.5$ in Eq. (1).[42] Submitting $n = 0.5$ and $\bar{\rho} \propto t/l$ into Eq. (2) derives $\bar{K}_{IC} \propto \bar{\rho}^{-1}$, this negative scaling parameter -1 is remarkable since it indicates that ultra-tough lattice materials can be achieved at a ultra-lower relative density.

Moreover, the pattern transformation induced by local buckling near the crack tip of a lattice material is analogous to the phase transformation (from tetragonal particle to monoclinic particle) in zirconia ceramics [Fig. 2(b-iv)].[56] Recall that in transformation-toughened zirconia, an optimal metastable tetragonal phase lays the key to strong and tough ceramics. Similarly, to generate "transformation-toughened" lattices, lattice geometries with low buckling stress (with low connectivity) are desired to trigger pattern transformation by the crack tip stress field. In particular, the stress that triggers local buckling (σ^B_{eff}) should be smaller than that causes a fracture (σ^F_{eff}), $\sigma^B_{eff} < \sigma^F_{eff}$, and σ^B_{eff} should be as larger as possible to improve the strength.

So far, we have introduced several mechanisms to toughen lattice materials and shown that low relative density may be critical to ultra-tough lattice metamaterials. Currently, lattice materials with ultra-high specific toughness have not been obtained, future researches of ultra-tough lattice materials may benefit by considering (1) hierarchical design that takes the most advantage of Eq. (2), (2) novel lattice topology for optimal transformation-toughening that provides significant crack blunting and large FPZ, and (3) heterogeneous lattices analogous to bio-inspired composites[57,58] [Fig. 3(c)] for extensive micro-cracking.

2. Lattice metamaterials that break performance trade-offs

Different properties of bulk materials are often closely correlated and thus difficult to improve together, notoriously known as the material performance trade-offs [Fig. 3(a)]. For instance, strong materials are typically less tough, stiff materials tend to be less dissipative, and flexible materials often recover slowly, just to name a few. Free combinations of material properties going beyond performance trade-offs are highly desired in nearly all engineering disciplines. In fact, performance trade-offs are the major obstacles for filling the "blank areas" on Ashby's plots.[59] Architected materials, with ingenious unit cell designs, open the door to (weakly) decouple different material properties and exceed performance trade-offs.

In the past decades, many architected materials have been developed to overcome the performance trade-offs. For example, metals with controlled grain distribution,[60] metallic glasses with shear band arresting dendrites,[61] and 3D printed composites with architected microstructures[62,63] have been developed to overcome the trade-off between strength and toughness. Staggered and co-continuous composites have been shown to make stiff materials more dissipative.[64–67] Hierarchy is shown to improve thermal resistance and stiffness, strength simultaneously.[68] More recently, a comprehensive study have summarized the efficient role of material architecture in breaking multiple performance trade-offs between strength, toughness, flexibility, dissipation, and fast response [Fig. 3(b)].[69]

Adapting the above design motifs of architected composites[61,64,66,68,69] to the design of lattice materials may analogously produce heterogeneous lattice materials that break performance trade-offs. The key feature of the architected composites, i.e., microstructures comprised of a stiff phase and a soft phase,[61,69] can be achieved equivalently by using different lattice geometries. One example is demonstrated in Fig. 3(b), where lattice structures with high and low relative density serve as the stiff and soft phase, respectively. Specifically, lattices with curvy geometry can be utilized as a soft phase with a large failure strain. More lattice geometries, e.g., triangular lattices are isotropic and stiffer, and square lattices are strongly anisotropic and weak to shear, can be used to obtain various effective properties.[68,70,71]

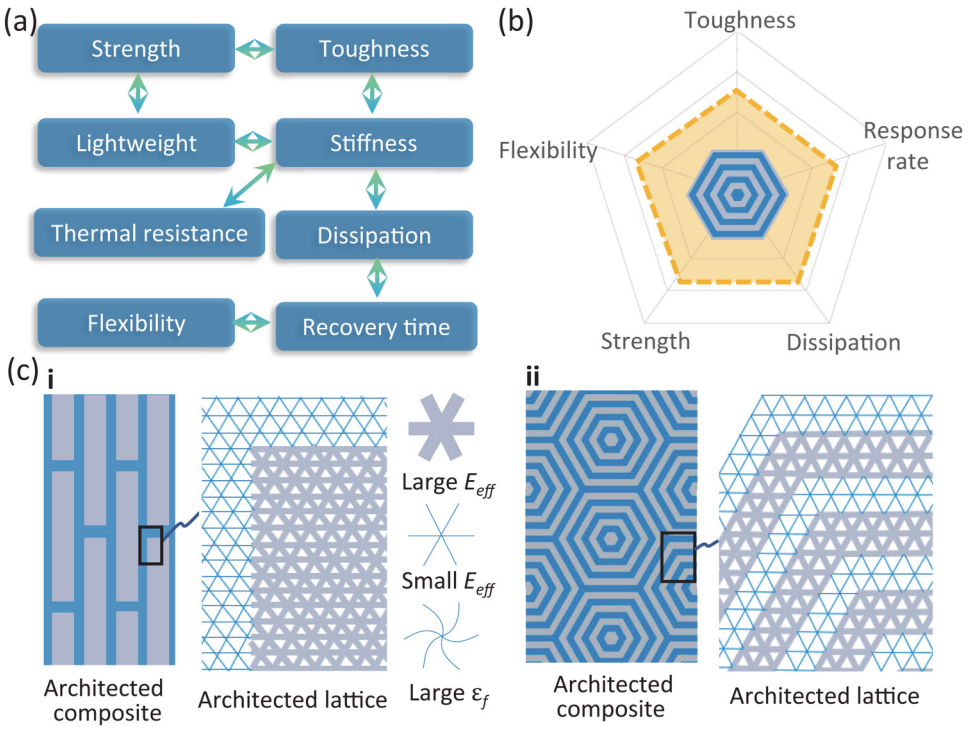

FIG. 3. Lattice metamaterials that break performance trade-offs. (a) Performance trade-offs in material sciences. (b) The concentric hexagonal microstructure possesses a balanced performance profile overcoming multiple trade-offs.[69] (c) Heterogeneous architected lattice materials based on architected composites. E_{eff} is the effective modulus of the unit cell and ϵ_f is the failure strain of the unit cell.

3. Lattice metamaterials with unusual properties

Conventional materials typically have positive material indices, and those with negative material indices are named as metamaterials. Our attention here focuses on the application of lattice metamaterials. In particular, we will discuss metamaterials with negative material indices[72,73] and phononic bandgap (Fig. 4 and Table I). Other lattice metamaterials, e.g., pentamode metamaterials,[74] photonic crystals,[75] topological metamaterials,[76] and non-reciprocal metamaterial[77] can be found in the corresponding references.

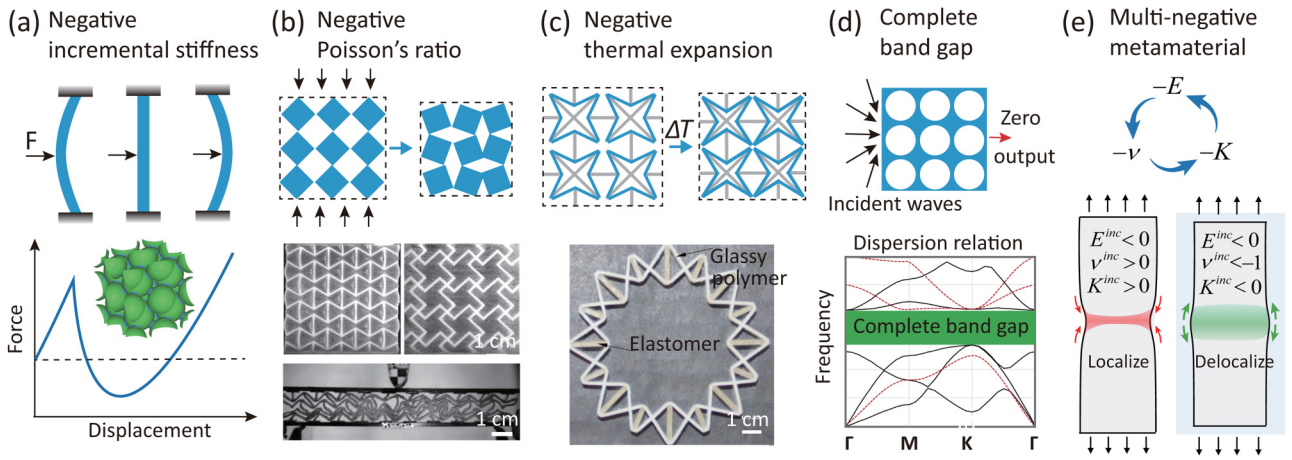

FIG. 4. Lattice metamaterials with unusual properties. (a) Negative incremental stiffness. (b) Negative Poisson's ratio. Images reproduced with permission from Li *et al.*, Mater. Des. **142**, 247–258 (2018) and Hou *et al.*, Mater. Design **160**, 1305–1321 (2018). Copyright 2018 Elsevier. (c) Negative thermal expansion. Image reproduced with permission from Y. Li, Y. Chen, T. Li, S. Cao, and L. Wang, Compos. Struct. **189**, 586–597 (2018).[167] Copyright 2018 Elsevier. (d) Phononic bandgap. (e) Considering multiple material indices in a coupled manner could give rise to novel lattice metamaterials. Reproduced with permission from Jia and Wang, Phys. Rev. Appl. **12**, 024040 (2019). Copyright 2019 American Physical Society.

TABLE I. Summary of the potential applications of lattice metamaterials with unusual properties.

Property	Applications
Negative stiffness	Energy absorption, extreme-sensors, extreme-damping
Negative Poisson's ratio	Indentation protection, reduce surface wrinkling, improve pull-out resistance
Negative thermal expansion	Zero thermal expansion, thermal stress-free materials
Phononic bandgap	Phononic switches, flexible phononic cloaks, thermal insulators
Multi-negative indices	Stable negative stiffness materials, unbounded negative Poisson's ratio, deformation delocalization

Figure 4(a) presents a typical force–displacement curve of a pre-curved beam element with negative incremental stiffness, where stress drops after reaching a critical value. A combination of multiple such peaks forms a serrated curve; therefore, an assembly of negative stiffness elements can be used for high energy absorption with controlled maximum force.[78] More interestingly, negative stiffness materials (NSMs) assist deformation (have negative deformation resistances) at applied force. Therefore, NSMs can undergo extensive deformation at even a small applied load.[79] Such a deformation amplification mechanism makes negative stiffness elements' perfect components to achieve extreme-damping when embedded in a viscoelastic matrix.[80–82] Besides, the amplification mechanism is analogous to power amplifiers in electronics which could be used to design extreme-sensitive mechanical sensors and ultra-low force triggered actuators.

On the other hand, the Reuss model writes the effective stiffness of a composite as

$$\frac{1}{E_{eff}} = \frac{V_1}{E_1} + \frac{1 - V_1}{E_2}. \tag{3}$$

From this equation, if there E_1 is negative and E_2 is positive, then by tuning the volume fraction of one phase, V_1, we can get zero on the right hand side, which means $E_{eff} \to \infty$. This indicates that in theory, an ultra-stiffness composite can be made using NSMs. However, the realization of this concept is hindered by the difficulty in making NSMs stable. We recently demonstrated that a triple-negative material is stable under displacement constraint, providing one approach to solve this dilemma.[44]

Next, let us turn our attention to the application of negative Poisson's ratio (NPR) and negative thermal expansion (NTE). NPR has been demonstrated in lattice materials with reentrant,[83] chiral,[70] and kirigami[84] structures [Fig. 4(b)]. Because NPR materials contract (become denser) under compression, they are advantageous to improving indentation resistance[85] and restraining compression induced wrinkles. Moreover, they can also improve fiber pull-out resistance[86] and improve structure recovery under impact.[87] NTE, on the other hand, can be adapted to design thermal stress-free ceramic lattices in jet engines.[73,88,89] Similar designs can also be utilized in satellite components that experience significant temperature changes during day and night, as well as high precision devices where the thermal deformation should be minimized.

In addition, phononic metamaterials are characterized by one or more frequency ranges where waves cannot propagate through [Fig. 4(d)]. This feature enables a broad range of applications, including perfect mirrors,[90] filters,[91] and waveguides.[92,93] Current research, on the one hand, is trying to make the bands tunable and, on the other, is trying to make the bandgap robust toward manufacture uncertainty and external perturbation. For instance, several deformation-controlled phononic switches have been proposed.[43,94] Phononic crystals with wide and robust bandgaps were achieved by the combination of Bragg scattering, local resonances, and instability suppression.[95] Lattice materials may found future phononic applications like thin layer materials for noise and vibration control,[70,96] flexible/deformable phononic devices,[95] lightweight acoustic cloaks,[97–99] and thermal insulators.[100,101]

So far, each material parameter is discussed separately. Deeper insights could be obtained if we consider multiple material indices simultaneously. As an example, let us consider the relation between Young's modulus (E), shear modulus (G), bulk modulus (K), and Poisson's ratio (ν) of isotropic materials. For isotropic materials to be stable under displacement constraint, these parameters should satisfy the inequalities summarized in Table II.[44,102] While most studies focus on region 1 or region 3, it is found that in region 2, E, K, and ν are all negative yet the material is stable. By contrast, an isotropic material with $E < 0$ but $K > 0$, $\nu > 0$ is unstable. This fact—multiple negative indices, instead of a single one, must be achieved simultaneously to guarantee stability—is ignored in previous searching of stable negative stiffness materials. In light of this, we have recently demonstrated a conceptual design that achieves triply negative E, K, and ν by tailoring snap-through instability.[44] Moreover, in region 2 (see Table II), no lower bounds exist for E and ν. Thereby, extreme E and ν values approaching negative infinity exist theoretically. This has been verified by simulation,[44] but direct experimental observation is prevented by a narrow tri-negative parameter region and defect sensitivity. Nevertheless, we believe similar considerations, treating multiple negative indices in a coupled manner, will benefit the discovery of both new metamaterials and new physics.

4. Lattice metamaterials with tailored stress–strain response

The development of materials is gradually transferring from "available materials" toward "tailored materials" that should satisfy

TABLE II. Parameter spaces of stable isotropic materials under displacement constraint.

Region 1, negative ν	Region 2, triple-negative	Region 3, negative K
$G > 0$	$G > 0$	$G > 0$
$E > 0$, $-1 < \nu < 0.5$	$E < 0$, $\nu < -1$	$E > 0$, $\nu > 1$
$K > 0$	$-G/3 < K < 0$	$-4G/3 < K < -G/3$

customized property requirements. Designing unit cells and their distribution provides a well-acknowledged approach to tune the effective properties of lattice materials.[3] This approach has been used by both engineers and researchers for a long time. While traditional studies focus on single-point properties like stiffness and Poisson's ratio, recent advances in machine learning (ML) and artificial intelligence have enabled us to tailor the nonlinear performance and even the whole stress–strain curve of a lattice material.[12–14]

To produce lattice materials with customized stress–strain curves, mechanisms that can achieve stress–strain curves of different shapes should be first identified. Some applicable structural features and mechanisms are depicted schematically in Fig. 5(a). Note here that the curves are phenomenologically divided into an initial linear elastic region followed by a nonlinear response for concept demonstration.

The proposed structure features in Fig. 5(a) can be designed to form a library of unit cells targeting different shapes of stress–strain responses. Once we have constructed a unit cell library that has a wide design space of stress–strain shapes, $\sigma(\varepsilon)$, an ML scheme can then be applied to customize the $\sigma(\varepsilon)$ curve based on certain design requirements [Fig. 5(b)]. The essential ingredients of an ML scheme are (1) model the design space as structure identification vectors, (2) model the stress–strain responses as property vectors and calculate a dataset for training, and (3) use ML models to correlate the relationship between structure vectors and property vectors. In the first step, the structure of lattice materials should be modeled mathematically. Lattice materials are assemblies of one or different types of unit cells; therefore, the structure identification vectors of a lattice material can be described utilizing a coarse grain approach,[12] i.e., each unit cell can be described by an identification vector as $\mathbf{I}_{cell}(N; E, \nu, \sigma_f; S_1, S_2, S_3, \ldots)$, where the first number describes the unit cell type, the following three parameters describe the material properties, and S_i are parameters that define the unit cell geometry. Moreover, a second structure matrix $\mathbf{I}_a$ of dimension $n \times n$ is required to describe the assembly of $n \times n$ unit cells into a lattice material. Second, a dataset for training should be produced. Specifically, lattice materials will first be constructed by assembling different unit cells randomly, and then, their stress–strain curves, $\sigma(\varepsilon)$, will be calculated using finite element analysis (FEA). The resultant curves can be represented as property vectors that save stress values at predefined strain points $\sigma(\varepsilon_i)$. Third, with structure fully defined by identification vector and training datasets obtained by FEA, ML models can be trained using methods like linear classification model,[103] support vector machine,[104] and convolutional neural network (CNN).[105] Once the ML model has accurately learned the underlying relationship between the identification vectors and the property vectors, it can finally be used to produce designs of lattice materials using customized $\sigma(\varepsilon)$ as input.

Here, we have summarized a general approach to tailor the stress–strain responses of lattice materials using ML. It should be pointed out that the continuity between different unit cells, the reduction of the vector length, and the simplification by using reduced-order modeling should also be considered for higher accuracy and computation efficiency. Moreover, the extension of the present 2D scheme to 3D is also of fundamental importance for future research.

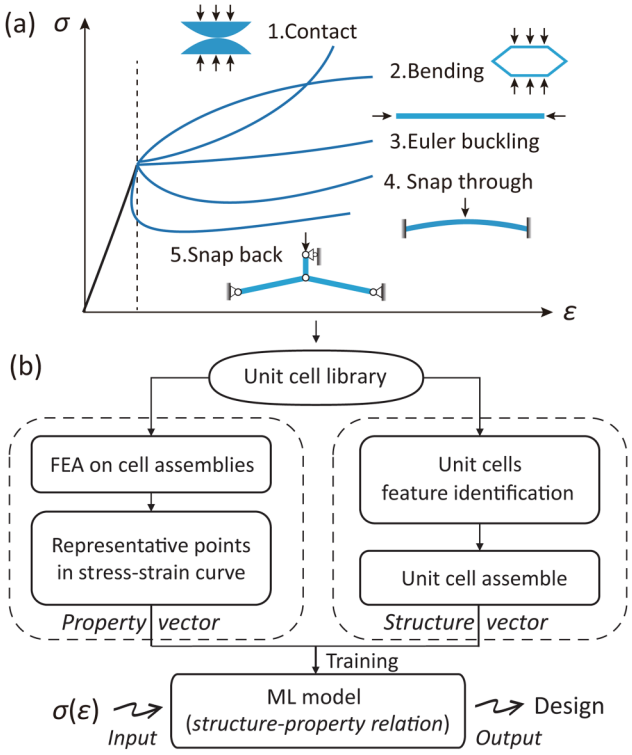

FIG. 5. (a) Structural features and mechanisms that can generate different nonlinear stress–strain responses. (b) A machine learning scheme utilized to customize stress–strain curves.

B. Programmable lattice metamaterials

In stark contrast to the extreme lattice materials discussed above, adaptive programmable materials possess unique architectures that can maintain, respond, and change their shapes and properties when subjected to external stimulations such as alternation in moisture, temperature, pressure, and external load. As depicted in Fig. 6(a), a programmable material typically has multiple stable states, and different material functions are programmed by switching between different stable states with certain controlling stimulation. The early concept of programmable materials is proposed in drug delivery systems, where programmed polymer structures can encapsulate/deploy under the change of temperature or pH [Fig. 6(b)].[106] More recently, instability is exploited to achieve multiple stable material topologies and tailor large deformation responses [Fig. 6(c)], opening new doors to design programmable lattice materials for more complex functions.[45,107,108] Examples include Kiri-kirigami sheets with notches to control light transmitting,[109] biholar sheets with lateral confinements to adjust stress–strain response,[110] and aperiodic, frustration-free architectures that can morph into complex shapes.[111] Aside from designing programmable materials by changing the

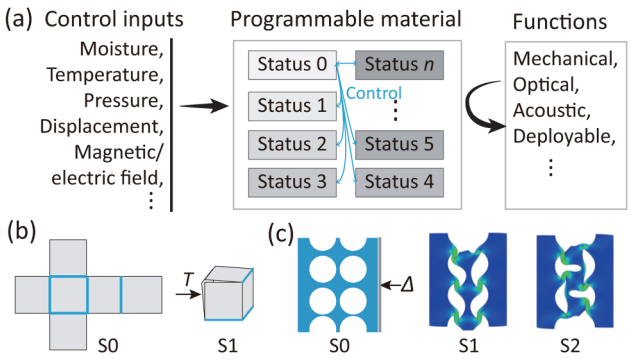

FIG. 6. Programmable materials. (a) A programmable material has multiple stable states; different functions are programed by switching between different states utilizing certain control. Examples of programmable metamaterials that switch states under (b) external temperature change and (c) applied load.

geometry of building blocks, programmability can also be achieved by changing the spatial distribution of materials. Such designs result in different types of instability modes that can be used for load switching, kinematic control, and grasping.[112]

The programmable materials mentioned above are pre-programmed, meaning that once designed and fabricated, the response of these materials cannot be changed because their programmability directly comes from the specially designed geometry. Post-programmed materials, on the other hand, refer to a new concept of programmable material, where the material is programmed after fabrication, thus greater freedom of programmability can be expected. One approach to design post-programmed materials is by controlling the boundary conditions of a well-designed lattice material, where different responses are programmed by changing the boundary conditions. Under this design motif, we will demonstrate two concepts of post-programmed metamaterials in the following.

Our first example is a lattice material composed of an array of pre-curved beams which can be post-programed by controlling the loading path. As shown in Fig. 7(a), a pre-curved beam (S0) can buckle into two different configurations under compression, namely, a local stable status S1 and an overall stable status S2. If we start with the compressed status S1 and do an "unloading–reloading operation" [Fig. 7(b)], i.e., gradually release the compression and then recompress the beam again, then two possible end statuses can be reached. Specifically, when the released displacement Δ exceeded a critical value Δ_{cr}, snapping will take place, changing

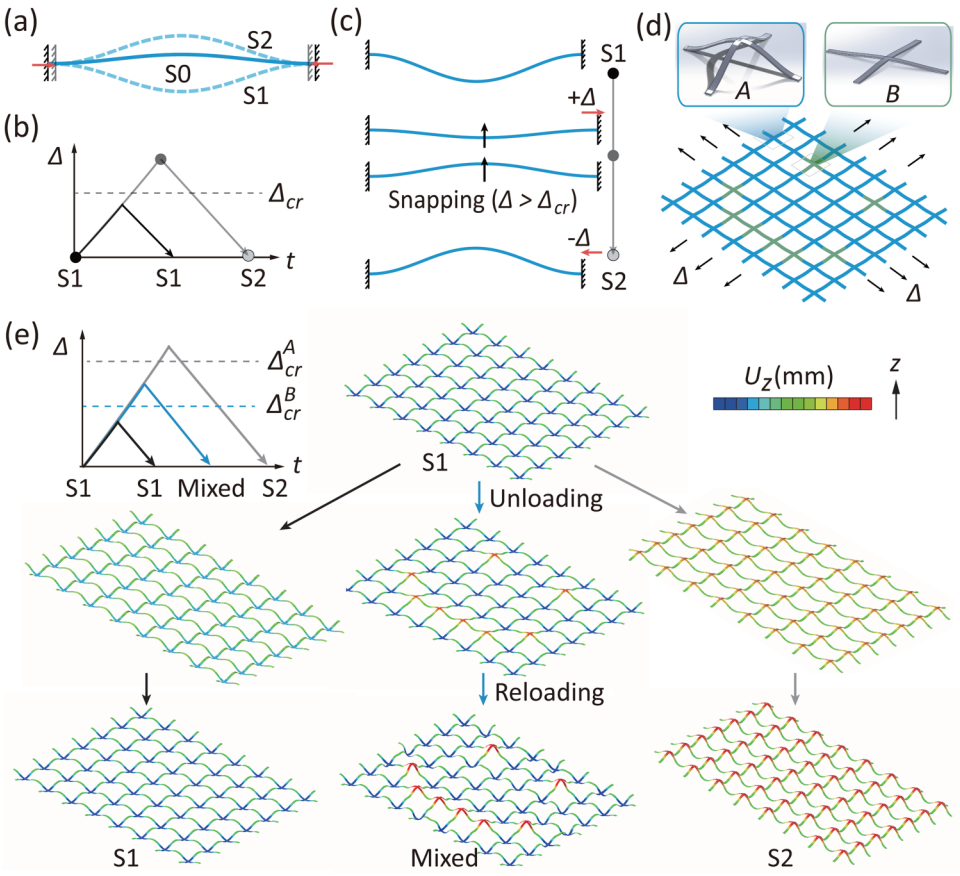

FIG. 7. A loading path controlled programmable lattice metamaterial. (a) A pre-curved beam S0 has two stable buckled statuses, S1 and S2. (b) An "unloading–reloading operation" can change the status of the pre-curved beam from S1 to S2 if the displacement is larger than a critical value $\Delta > \Delta_{cr}$. (c) Snapping takes place at $\Delta > \Delta_{cr}$ and changes the configuration of the beam. (d) The design of a post-programmed lattice material using elements of type *A* and type *B* (not drawn to scale). (e) Different structure configurations programmed utilizing different loading paths. Specifically, a smiling face is obtained in the second loading path with blue color.

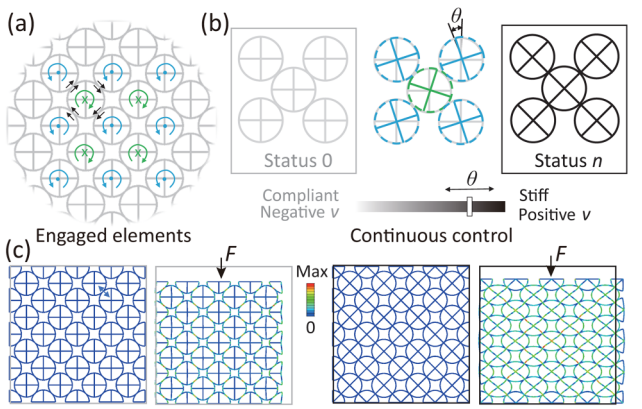

FIG. 8. A lattice metamaterial with continuously programmable stiffness and Poisson's ratio controlled by angle of rotation θ. (a) A programmable material analogy to an engaged gear system. (b) Continuously controllable Young's modulus E and Poisson's ratio ν. (c) Deformations under compression at status 0 (left) and status n (right), demonstrating negative ν and positive ν, respectively.

the beam from status S1 to status S2 as depicted in Fig. 7(c). By contrast, when the released displacement is small enough ($\Delta < \Delta_{cr}$), the original S1 status can be maintained after the unloading–reloading operation. As such, different end status can be programmed by different "unloading–reloading" operations. Using this mechanism, lattice materials with an increasing number of programmable status can be designed by assembling a large number of such pre-curved beams. Figure 7(d) presents an example design composed by 2D pre-curved beams using elements of type A and type B. Specifically, elements of type A have a greater pre-curvature than elements of type B and, thus, also has a larger critical snapping curvature $\Delta_{cr}^{A} > \Delta_{cr}^{B}$. Harnessing this feature, different shapes of the lattice can be programmed using different loading paths [Fig. 7(e)]. Particularly, for the loading with $\Delta_{cr}^{B} < \Delta < \Delta_{cr}^{A}$, elements of type B reach the critical points and snap upward while elements of type A do not, which forms a smiling face. Obviously, when more controls on the distribution of loading displacement on the lattice boundary are introduced, more intricate deformation patterns can be expected.

Most programmable materials possess discrete stable statuses; our second example demonstrates a programmable lattice material with continuous stable statuses. The material concept is demonstrated in Fig. 8, which is a 2D lattice material composed of engaged cylinders with cross reinforcement inside. All the elements are engaged such that the rotation of a single element (θ) changes the configuration of the whole lattice material from status 0 to status n [Fig. 8(b)]. The lattice material is designed such that the performance of status 0 has a great performance difference to that of status n. Simulation results show that the lattice material is compliant and has a negative Poisson's ratio at status 0 [Fig. 8(c)]. By contrast, the lattice material becomes much stiffer and possesses a positive Poisson's ratio at status n. As such, by varying the angle of rotation θ, the proposed lattice material achieves continuously programmable stiffness and lateral expansion.

C. Multifunctional lattice metamaterials

Multifunctional materials achieve various functions with a single material, thus can save raw material and reduce structure weight.[113,114] Multifunctionality can be constituent-based or structure-based. Examples of constituent-based multifunctional materials are carbon nanotube/graphene,[115–117] piezoelectric materials,[118–120] and shape memory materials,[121–123] which can achieve catalytic, energetic, and adaptive performances. These cutting-edge constituent-based materials, however, have disadvantages: (1) they are relatively expensive and (2) their functions arise from constituents, therefore, the design is material dependent and cannot be generalized for other materials.

The above two disadvantages can be addressed straightforwardly by the structure-based multifunctional materials. As indicated by the name, structure-based multifunctional materials derive their multifunctionality from microstructure, like architected materials.[2] As such, cheap material constituents can be used straightforwardly. More important, the unlimited constituents together with the large freedom in 3D microstructure design offer an extremely wide design space, when compared to that of the constituent-based counterparts. Because the exceptional mechanical, thermal, and acoustic properties of lattice metamaterials are dominantly by the lattice structure,[3,114,124] their multifunction is often structure-based.

Here, we utilize periodic hollow sphere foam (HSF) as an example to illustrate the multifunctionality of lattice metamaterials (Fig. 9). Some impressive performances and functions achieved by HSF include but are not limited to the following:

(a) Lightweight (general requirement, especially important for transport systems).
(b) Large void space (provides buoyancy and enable pressure-controlled actuation).
(c) Large specific area (heat radiator and catalyst support).
(d) Low thermal conductivity (thermal insulation).
(e) Negative Poisson's ratio (mechanical diode and energy absorption).
(f) Negative stiffness (produce extreme-stiffness and extreme-damping composites).
(g) Negative compressibility (mechanical actuator).
(h) Phononic bandgap (wave propagation control and wave mitigation).

The first four functions are common features of cellular materials and, thus, can be categorized as intrinsic properties of lattice materials. Nevertheless, special considerations should be given. First, to design a lightweight structure, not only high porosity but also high stiffness and strength should be accomplished, as a light but weak material is not too useful. In this case, a linear scaling between stiffness and strength is appreciated [Fig. 9(b)]. Second, there is a trade-off between large void space and large specific surface area in lattice materials. Because when more volumes are closed to form voids, the exposed surface area is reduced. Specifically, fully open-cell lattices and fully closed-cell lattices [Fig. 1(a)] are the two limiting cases. HSF lies at the intermediate of these two limits, balancing a large void space and a large surface area. Third, Fig. 9(c) plots the effective thermal conductivity of HSF with the spherical shells made of glass. Low K_{eff} comparable to air can be readily obtained. To

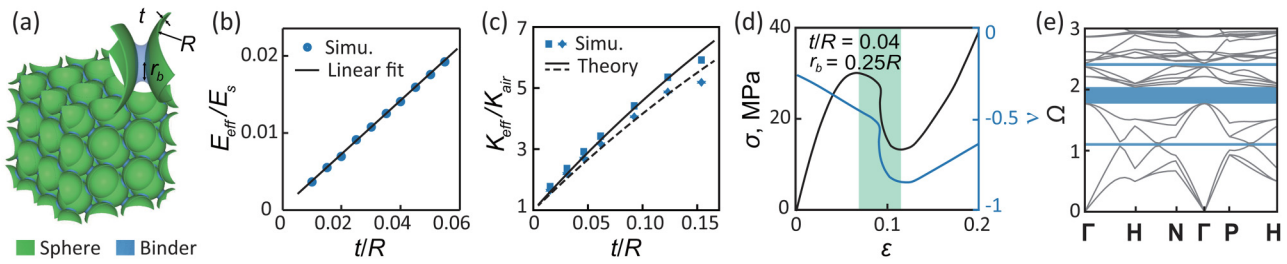

FIG. 9. A multifunctional lattice metamaterial. (a) Structure. r_b is the binder radius, R and t represent sphere radius and thickness, respectively. (b) Linear scaling enables high specific stiffness and specific strength, (c) low thermal conductivity comparable to air, (d) triple-negative material indices (the material exhibit negative E, ν, and K in the highlighted strain range), and (e) phononic bandgap enables wave propagation control. Dimensions: (b) $r_b = 0.3R$ and (c) the square represents $r_b = 0.3R$, and the diamond represents $r_b = 0.2R$.

reduce the thermal conductivity further, additional modifications include: (1) fill the voids with low conductivity gas, (2) use a smaller cell size to take advantage of the Knudsen effect, and (3) develop second-order porous shell to improve overall porosity.[125]

The latter four properties, in contrast, are not natural outcomes of lattice materials—they must be obtained through rational designs and, thus, can be categorized as extrinsic functions. As discussed in the metamaterial section, a large number of lattice structures have been shown to possess negative Poisson's ratio, e.g., re-entrant, chiral, kirigami, and origami. Lattice materials with a negative Poisson's ratio can thus be achieved by introducing these structural features. By contrast, the design of negative stiffness is more challenging due to the stability constraint. In particular, negative stiffness should be considered in couple with a negative Poisson's ratio and negative compressibility [Fig. 9(d)], because a stable negative stiff material (under displacement constraint) must be triple-negative.[44] Finally, to further add the wave attenuation ability to lattice materials, two design paradigms can be considered: highly symmetric lattices and lumped lattices.[95] Recent developments in topological optimization also provide an efficient approach to achieve these extra extrinsic functions.[126,127] The existence of phononic bandgap in HSF is demonstrated in Fig. 9(e), more extensive discussions can be found in Ref. 128.

In addition to the above-demonstrated functions, functions like high material toughness, optical performance, and reconfigurable function can further be envisioned in HSF. Specifically, approaches to designing tough lattice materials have been discussed in Sec. II A. Photonic functions can be expected when the lattice is scaled to a sub-micrometer size.[46]

While our discussion here focuses on structure-based material functions, it is important to note that the constituent-based multifunctionality should be treated of equal importance. Significant progresses have been made in the material–function relationship recently. In particular, novel materials like carbon-based nanocomposites,[129] electroactive polymers,[130] piezoceramics,[131] shape memory materials,[121] ferromagnetics,[132] and opto-chemical sensitive materials[133] can further enabled stress, thermal, electric, magnetic, light, and molecular responsive functions. An integration of the above constituent-based function with a structure-based function will greatly enrich the function library of lattice materials and enable fancy applications like self-healing, self-powered material systems,[113] autonomous sensing, and actuating systems.[114,134,135] For example, when thermoelectric materials, carbon nanotubes, and piezoelectric nanowires are utilized to build lattice materials, energy harvesting, sensing, and self-powering functions can be introduced readily.[136,137] To achieve this, multimaterial 3D printers and new print-ink designs are of special research interest. Some recent achievements in fabrication include the development of piezoelectric inkjet printers,[138] multimaterial multinozzle 3D printers,[23] ferromagnetic particle imbedded elastomer inkjet printers,[139] and fiber direction controlled 3D printers.[140] As the research on functional materials, fabrication techniques, and lattice structure design go on, no doubt more functions and novel applications of lattice metamaterials will be discovered in the future.

III. METHODOLOGIES FOR LATTICE METAMATERIAL DESIGN

From a more general perspective, lattice materials are quite ubiquitous not only in the context of engineering lattice metamaterials we have discussed so far but also in bulk materials down to the atomic scale, in biomaterials with hierarchy and gradient, and in architectures at a larger (10–100 m) scale (Fig. 9). These various systems have formed a resource-rich library of lattice structures; among them, plenty of smart and inspiring designs can be found. In this section, we will highlight different design methodologies of lattice materials used by mother nature, our fellow material scientists, and fellow engineers.

In biological systems, natural selection prefers robust structure designs that consume the least material and energy. As cellular materials have a high structure efficiency, nature has evolved numerous lattice-like structures, examples include insect wings, bamboos, bones, sea sponge, and sea star ossicles. Hierarchy and structural gradient are two well-known features of biological materials [Fig. 10(a)] that enable the use of a single material (like biogenic ceramics) to satisfy both structural and functional needs. Hierarchy generates microstructures at multiple length scales while gradient controls the spatial distribution of materials. A combination of these two features produces impressive mechanical, environment responsive, and multifunctional properties.[141,142] Besides hierarchy and

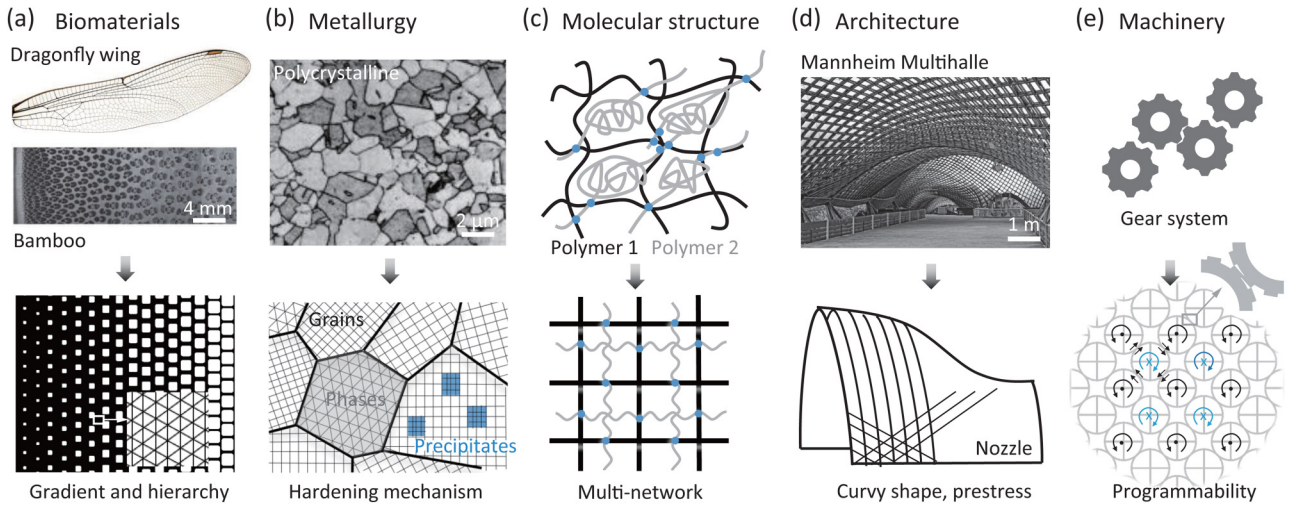

FIG. 10. Design methodology of lattice materials inspired from (a) nature, (b) and (c) material sciences, and (d) and (e) engineering. The picture in (a) is reproduced with permission from Mannan *et al.*, R. Soc. Open Sci. **4**, 160412 (2017). Copyright 2017 The Royal Society.[165] The picture in (d) is reproduced with permission from P. Nicholas, E. L. Hernández, and C. Gengnagel, *The Faraday Pavilion: Activating Bending in the Design and Analysis of an Elastic Gridshell* (SimAUD, 2013). Copyright 2013 SimAUD.[166]

gradient, we here emphasize another important feature, structural randomness, of biological materials. From cancellous bones to sea urchin spines,[143,144] nearly all lattice materials in nature have a certain level of structural irregularity,[3] in sharp contrast to engineered periodic lattices. Although it might be true that organisms do not intentionally grow irregular lattices, we highlight that a proper level of structure randomness can be beneficial.[145] Previous studies have shown that randomness can improve strength (>10%) by eliminating the natural fault planes in ordered lattices.[146] By contrast, study on random Voronoi honeycombs reveal that fracture toughness decreases at increasing level of randomness.[147] However, this study have not took the crack propagation into consideration. Our recent study reveals that adding structure randomness to a periodic lattice forms a more tortuous crack path and facilitates a more progressive fracture process and, thus, can potentially dissipate more energy although at the expense of mildly reduced stiffness. Besides, random lattices can improve biological compability,[146] making geometric randomness specially importance for biomedical lattice materials. Note that randomness in biological materials is often limited to the statistical variations of the unit cell geometry and are nearly defect-free.[148] This feature is different to 3D printed lattice materials where defects may exist at the material level (cracks induced during cure), strut level (waviness and uneven thickness),[149] and unit cell level (vacancy and inclusion).[150] In addition to the two well-recognized research directions of bio-inspiration, i.e., optimal hierarchical design (flaw tolerance at all levels)[141,151] and functional gradient design,[152] research on lattice material designs may also benefit by investigating how nature takes advantage of structural randomness yet reduces the structural defects.[153]

On the other hand, material scientists have been playing with material microstructure for centuries. Lattice materials on a macroscopic scale are analogous to the crystal microstructure of metals and alloys at the atomic level. For example, a single crystal is prone to localized shear in certain glide planes and known to be weak in metallurgy,[154] similarly, directional weakness is also found in periodic lattice materials.[155] In light of this analogy, hardening mechanisms inspired by crystallography, i.e., grain boundaries, precipitates, and multiphase strengthening have been successfully used to improve the damage tolerance of engineered lattice materials [Fig. 10(b)].[155] Besides metallurgical concepts, other materials like shape memory polymers/alloys,[122,156] stretchy and tough hydrogels,[157] and transformation-toughened ceramics[56] can also inspire new lattice material design motifs. For instance, some polymers possess large deformation and shape memory effect due to the existence of a weak but recoverable elastomer network. A lattice material concept that mimics this mechanism is a two-grid lattice material [Fig. 10(c)], where weak networks are represented by wavy branches. This polymer-inspired lattice material can recover its original shape even after the break of the strong network (straight branches). When further combined with external healing mechanisms, a macroscale shape memory and self-healing macroscale lattice material could be obtained straightforwardly.

In engineering, architects and mechanical engineers have also devoted much effort to design lattices or lattice-like structures. For example, buildings like pillarless stadiums and domes are often constructed by lattice structures [Fig. 10(d)]. Such curvy shaped buildings are not only visually pleasing but also stiff, easily-repairable, and lightweight. Similar designs can be used to produce 3D curvy lattice materials for applications like engine nozzles and drone frameworks. Moreover, analogous to the generation of a 3D tent by bending 2D frames, researchers have fabricated curvy lattices by compressing flat sheets.[158] In parallel to architecture, mechanical engineering is another old engineering discipline, where machines consist of multi-movable structural components. Specifically, executable components

in machinery are desired in actuatable lattice materials, which can inspire the design of programmable lattice metamaterials. For instance, a gear system inspired lattice material with tunable stiffness and Poisson's ratio is shown in Fig. 10(e). Potentially, other mechanical mechanisms like linkage and cam can also provide useful insights into the design of actuation lattice materials.

The above design approaches may produce lattice metamaterial designs with complex designs that are challenging to fabricate, even for state of the art 3D printing techniques. Example include lattice materials with hierarchy similar to biomaterials, lattice materials with enclosed cells, and lattice materials with movable components. To solve these challenging requirements, novel fabrication approaches are envisioned. Considering recent advances in both 3D printing (μm – mm)[18,21,23] and self-assembly techniques (nm – μm),[159–161] successful combinations of these two approaches may expand the manufacturable space of lattice metamaterials to satisfy most engineering need.[162–164]

IV. CONCLUSION

Lattice metamaterials not only facilitate the development of low-density materials with unusual and tailorable properties but also open the door to smart, adaptive, programmable, and multifunctional materials. In this perspective, we have discussed the design strategies, provided examples, and identified future research opportunities for three emerging research directions of lattice metamaterials: (1) extreme lattice materials with exceptional mechanical properties, tailored properties breaking performance trade-offs, and multiple negative properties; (2) programmable lattice metamaterials whose response or function can be post-programmed and switched seamlessly using external stimuli; and (3) multifunctional metamaterials that integrate a wide range of functions and, thus, are the ultimate lightweight and structure-efficient materials. While significant progress has been made in the lattice metamaterial design and fabrication, the realistic application still requires integrated design–modeling–experiment–optimization–manufacturing approaches, spanning material science, applied mechanics, computer science, and mechanical engineering. Advanced lattice metamaterials are poised to shape the future of materials, but a systematic paradigm should be sought to accelerate their development and take advantage of their full potential.

ACKNOWLEDGMENTS

This research was partly supported by the National Science Foundation (NSF) (No. CMMI-1462270). The authors acknowledge the use of the Center for Functional Nanomaterials facility at the Brookhaven National Laboratory.

REFERENCES

[1]E. M. K. Abad, S. A. Khanoki, and D. Pasini, Int. J. Fatigue **47**, 126 (2013).
[2]T. A. Schaedler and W. B. Carter, Annu. Rev. Mater. Res. **46**, 187 (2016).
[3]L. J. Gibson and M. F. Ashby, *Cellular Solids: Structure and Properties* (Cambridge University Press, 1997).
[4]M. F. Ashby, T. Evans, N. A. Fleck, J. Hutchinson, H. Wadley, and L. Gibson, *Metal Foams: A Design Guide* (Elsevier, 2000).
[5]A. G. Evans, J. W. Hutchinson, N. A. Fleck, M. Ashby, and H. Wadley, Prog. Mater Sci. **46**, 309 (2001).
[6]V. Deshpande, M. Ashby, and N. Fleck, Acta Mater. **49**, 1035 (2001).
[7]M. C. Messner, J. Mech. Phys. Solids **96**, 162 (2016).
[8]J. Berger, H. Wadley, and R. McMeeking, Nature **543**, 533 (2017).
[9]G. Milton, Nature **564**, E1 (2018).
[10]T. Tancogne-Dejean, M. Diamantopoulou, M. B. Gorji, C. Bonatti, and D. Mohr, Adv. Mater. **30**, 1803334 (2018).
[11]X. Zheng, H. Lee, T. H. Weisgraber, M. Shusteff, J. DeOtte, E. B. Duoss, J. D. Kuntz, M. M. Biener, Q. Ge, and J. A. Jackson, Science **344**, 1373 (2014).
[12]G. X. Gu, C.-T. Chen, D. J. Richmond, and M. J. Buehler, Mater. Horiz. **5**, 939 (2018).
[13]Z. Liu, C. Wu, and M. Koishi, Comput. Method. Appl. Mech. Eng. **345**, 1138 (2019).
[14]C. Yang, Y. Kim, S. Ryu, and G. X. Gu, Mater. Des. **189**, 108509 (2020).
[15]D. J. Sypeck and H. N. Wadley, Adv. Eng. Mater. **4**, 759 (2002).
[16]D. Sypeck and H. Wadley, J. Mater. Res. **16**, 890 (2001).
[17]S. Chiras, D. Mumm, A. Evans, N. Wicks, J. Hutchinson, K. Dharmasena, H. Wadley, and S. Fichter, Int. J. Solids Struct. **39**, 4093 (2002).
[18]D. A. Walker, J. L. Hedrick, and C. A. Mirkin, Science **366**, 360 (2019).
[19]M. P. de Beer, H. L. van der Laan, M. A. Cole, R. J. Whelan, M. A. Burns, and T. F. Scott, Sci. Adv. **5**, eaau8723 (2019).
[20]J. R. Tumbleston, D. Shirvanyants, N. Ermoshkin, R. Janusziewicz, A. R. Johnson, D. Kelly, K. Chen, R. Pinschmidt, J. P. Rolland, and A. Ermoshkin, Science **347**, 1349 (2015).
[21]B. E. Kelly, I. Bhattacharya, H. Heidari, M. Shusteff, C. M. Spadaccini, and H. K. Taylor, Science **363**, 1075 (2019).
[22]A. Hosny, S. J. Keating, J. D. Dilley, B. Ripley, T. Kelil, S. Pieper, D. Kolb, C. Bader, A.-M. Pobloth, and M. Griffin, 3D Print. Addit. Manuf. **5**, 103 (2018).
[23]M. A. Skylar-Scott, J. Mueller, C. W. Visser, and J. A. Lewis, Nature **575**, 330 (2019).
[24]T. A. Schaedler, A. J. Jacobsen, A. Torrents, A. E. Sorensen, J. Lian, J. R. Greer, L. Valdevit, and W. B. Carter, Science **334**, 962 (2011).
[25]J. Bauer, A. Schroer, R. Schwaiger, and O. Kraft, Nat. Mater. **15**, 438 (2016).
[26]R. E. Miller, Int. J. Mech. Sci. **42**, 729 (2000).
[27]V. S. Deshpande, N. A. Fleck, and M. F. Ashby, J. Mech. Phys. Solids **49**, 1747 (2001).
[28]W. Sanders and L. Gibson, Mater. Sci. Eng. A **352**, 150 (2003).
[29]H. Fan, D. Fang, and F. Jing, Mater. Des. **29**, 2038 (2008).
[30]K. Bertoldi, M. C. Boyce, S. Deschanel, S. Prange, and T. Mullin, J. Mech. Phys. Solids **56**, 2642 (2008).
[31]C. Coulais, J. T. Overvelde, L. A. Lubbers, K. Bertoldi, and M. van Hecke, Phys. Rev. Lett. **115**, 044301 (2015).
[32]H. Fan, F. Jin, and D. Fang, Mater. Des. **30**, 4136 (2009).
[33]M. S. Anderson and F. Williams, AIAA J. **24**, 163 (1986).
[34]F. Côté, N. Fleck, and V. Deshpande, Int. J. Fatigue **29**, 1402 (2007).
[35]B. Van Hooreweder and J.-P. Kruth, CIRP Ann. **66**, 221 (2017).
[36]M.-W. Wu, J.-K. Chen, B.-H. Lin, and P.-H. Chiang, Mater. Des. **134**, 163 (2017).
[37]I. Quintana-Alonso and N. A. Fleck, *Major Accomplishments in Composite Materials and Sandwich Structures* (Springer, 2009), p. 799.
[38]S. Maiti, M. Ashby, and L. Gibson, Scr. Metall. **18**, 213 (1984).
[39]H. Tankasala, V. Deshpande, and N. Fleck, J. Appl. Mech. **82**, 091004 (2015).
[40]M. O'Masta, L. Dong, L. St-Pierre, H. Wadley, and V. Deshpande, J. Mech. Phys. Solids **98**, 271 (2017).
[41]A. Cherkaev and M. Ryvkin, Arch. Appl. Mech. **89**, 485 (2019).
[42]N. A. Fleck and X. Qiu, J. Mech. Phys. Solids **55**, 562 (2007).
[43]P. Wang, F. Casadei, S. Shan, J. C. Weaver, and K. Bertoldi, Phys. Rev. Lett. **113**, 014301 (2014).
[44]Z. Jia and L. Wang, Phys. Rev. Appl. **12**, 024040 (2019).
[45]N. Kidambi, R. L. Harne, and K.-W. Wang, Phys. Rev. E **98**, 043001 (2018).
[46]K. R. Phillips, C. T. Zhang, T. Yang, T. Kay, C. Gao, S. Brandt, L. Liu, H. Yang, Y. Li, J. Aizenberg, and L. Li, "Fabrication of photonic microbricks via crack engineering of colloidal crystals," Adv. Funct. Mater. (published online 2019), article No. 1908242.
[47]K. H. Nam, I. H. Park, and S. H. Ko, Nature **485**, 221 (2012).

[48]M. E. Kolewe, H. Park, C. Gray, X. Ye, R. Langer, and L. E. Freed, Adv. Mater. **25**, 4459 (2013).
[49]X. Zhang, A. Vyatskikh, H. Gao, J. R. Greer, and X. Li, Proc. Natl. Acad. Sci. U.S.A. **116**, 6665 (2019).
[50]L. R. Meza, S. Das, and J. R. Greer, Science **345**, 1322 (2014).
[51]J. Morgan, J. Wood, and R. Bradt, Mater. Sci. Eng. **47**, 37 (1981).
[52]Z. P. Bazant and E.-P. Chen, Appl. Mech. Rev. **50**, 593 (1997).
[53]H. Gao, B. Ji, I. L. Jäger, E. Arzt, and P. Fratzl, Proc. Natl. Acad. Sci. U.S.A. **100**, 5597 (2003).
[54]D. Jang and J. R. Greer, Scr. Mater. **64**, 77 (2011).
[55]R. Lakes, Nature **361**, 511 (1993).
[56]E. Butler, Mater. Sci. Technol. **1**, 417 (1985).
[57]W. Clegg, K. Kendall, N. M. Alford, T. Button, and J. Birchall, Nature **347**, 455 (1990).
[58]Z. Jia and L. Wang, Acta Mater. **173**, 61 (2019).
[59]M. F. Ashby, Philos. Mag. **85**, 3235 (2005).
[60]X. Wu, M. Yang, F. Yuan, G. Wu, Y. Wei, X. Huang, and Y. Zhu, Proc. Natl. Acad. Sci. U.S.A. **112**, 14501 (2015).
[61]R. O. Ritchie, Nat. Mater. **10**, 817 (2011).
[62]F. Bouville, E. Maire, S. Meille, B. Van de Moortèle, A. J. Stevenson, and S. Deville, Nat. Mater. **13**, 508 (2014).
[63]E. Munch, M. E. Launey, D. H. Alsem, E. Saiz, A. P. Tomsia, and R. O. Ritchie, Science **322**, 1516 (2008).
[64]P. Zhang, M. A. Heyne, and A. C. To, J. Mech. Phys. Solids **83**, 285 (2015).
[65]J. Meaud, T. Sain, B. Yeom, S. J. Park, A. B. Shoultz, G. Hulbert, Z.-D. Ma, N. A. Kotov, A. J. Hart, and E. M. Arruda, ACS Nano **8**, 3468 (2014).
[66]R. Lakes, J. Compos. Mater. **36**, 287 (2002).
[67]L. Wang, J. Lau, E. L. Thomas, and M. C. Boyce, Adv. Mater. **23**, 1524 (2011).
[68]Y. Chen, Z. Jia, and L. Wang, Compos. Struct. **152**, 395 (2016).
[69]Z. Jia, Y. Yu, and L. Wang, Mater. Des. **168**, 107650 (2019).
[70]Y. Chen, T. Li, F. Scarpa, and L. Wang, Phys. Rev. Appl. **7**, 024012 (2017).
[71]C. Schumacher, B. Bickel, J. Rys, S. Marschner, C. Daraio, and M. Gross, ACM Trans. Graph. **34**, 136 (2015).
[72]R. Lakes, Science **235**, 1038 (1987).
[73]O. Sigmund and S. Torquato, Appl. Phys. Lett. **69**, 3203 (1996).
[74]M. Kadic, T. Bückmann, N. Stenger, M. Thiel, and M. Wegener, Appl. Phys. Lett. **100**, 191901 (2012).
[75]C. Soukoulis, Nanotechnology **13**, 420 (2002).
[76]M. Z. Hasan and C. L. Kane, Rev. Mod. Phys. **82**, 3045 (2010).
[77]C. Coulais, D. Sounas, and A. Alù, Nature **542**, 461 (2017).
[78]S. Shan, S. H. Kang, J. R. Raney, P. Wang, L. Fang, F. Candido, J. A. Lewis, and K. Bertoldi, Adv. Mater. **27**, 4296 (2015).
[79]T. Klatt and M. R. Haberman, J. Appl. Phys. **114**, 033503 (2013).
[80]M. R. Haberman, M.S. thesis, Georgia Institute of Technology, 2007.
[81]R. Lakes, Phys. Rev. Lett. **86**, 2897 (2001).
[82]D. Chronopoulos, I. Antoniadis, M. Collet, and M. Ichchou, Wave Motion **58**, 165 (2015).
[83]B. Xu, F. Arias, S. T. Brittain, X.-M. Zhao, B. Grzybowski, S. Torquato, and G. M. Whitesides, Adv. Mater. **11**, 1186 (1999).
[84]Y. Cho, J.-H. Shin, A. Costa, T. A. Kim, V. Kunin, J. Li, S. Y. Lee, S. Yang, H. N. Han, and I.-S. Choi, Proc. Natl. Acad. Sci. U.S.A. **111**, 17390 (2014).
[85]T. Li, Y. Chen, X. Hu, Y. Li, and L. Wang, Mater. Des. **142**, 247 (2018).
[86]V. Simkins, A. Alderson, P. Davies, and K. Alderson, J. Mater. Sci. **40**, 4355 (2005).
[87]S. Hou, T. Li, Z. Jia, and L. Wang, Mater. Des. **160**, 1305 (2018).
[88]R. Lakes, Appl. Phys. Lett. **90**, 221905 (2007).
[89]Q. Wang, J. A. Jackson, Q. Ge, J. B. Hopkins, C. M. Spadaccini, and N. X. Fang, Phys. Rev. Lett. **117**, 175901 (2016).
[90]A. Khelif, B. Djafari-Rouhani, J. Vasseur, and P. Deymier, Phys. Rev. B **68**, 024302 (2003).
[91]M. Sigalas, J. Appl. Phys. **84**, 3026 (1998).
[92]A. Khelif, A. Choujaa, S. Benchabane, B. Djafari-Rouhani, and V. Laude, Appl. Phys. Lett. **84**, 4400 (2004).
[93]J. Vasseur, A.-C. Hladky-Hennion, B. Djafari-Rouhani, F. Duval, B. Dubus, Y. Pennec, and P. Deymier, J. Appl. Phys. **101**, 114904 (2007).
[94]S. Babaee, N. Viard, P. Wang, N. X. Fang, and K. Bertoldi, Adv. Mater. **28**, 1631 (2016).
[95]Z. Jia, Y. Chen, H. Yang, and L. Wang, Phys. Rev. Appl. **9**, 044021 (2018).
[96]L. Wang and K. Bertoldi, Int. J. Solids Struct. **49**, 2881 (2012).
[97]R. Fleury, F. Monticone, and A. Alù, Phys. Rev. Appl. **4**, 037001 (2015).
[98]S. A. Cummer and D. Schurig, New J. Phys. **9**, 45 (2007).
[99]X. Zhu, B. Liang, W. Kan, X. Zou, and J. Cheng, Phys. Rev. Lett. **106**, 014301 (2011).
[100]M. Maldovan, Nature **503**, 209 (2013).
[101]P. E. Hopkins, C. M. Reinke, M. F. Su, R. H. Olsson III, E. A. Shaner, Z. C. Leseman, J. R. Serrano, L. M. Phinney, and I. El-Kady, Nano Lett. **11**, 107 (2010).
[102]T. Jaglinski, D. Kochmann, D. Stone, and R. Lakes, Science **315**, 620 (2007).
[103]G. X. Gu, C.-T. Chen, and M. J. Buehler, Extreme Mech. Lett. **18**, 19 (2018).
[104]Y. F. Cao, W. Wu, H. L. Zhang, and J. M. Pan, *Prediction of the Elastic Modulus of Self-Compacting Concrete Based on SVM* (Trans Tech Publications, 2013), p. 1023.
[105]Z. Yang, Y. C. Yabansu, R. Al-Bahrani, W.-K. Liao, A. N. Choudhary, S. R. Kalidindi, and A. Agrawal, Comput. Mater. Sci. **151**, 278 (2018).
[106]X. Fan, J. Y. Chung, Y. X. Lim, Z. Li, and X. J. Loh, ACS Appl. Mater. Interfaces **8**, 33351 (2016).
[107]A. A. Zadpoor, Mater. Horiz. **3**, 371 (2016).
[108]B. Haghpanah, H. Ebrahimi, D. Mousanezhad, J. Hopkins, and A. Vaziri, Adv. Eng. Mater. **18**, 643 (2016).
[109]Y. Tang, G. Lin, S. Yang, Y. K. Yi, R. D. Kamien, and J. Yin, Adv. Mater. **29**, 1604262 (2017).
[110]B. Florijn, C. Coulais, and M. van Hecke, Phys. Rev. Lett. **113**, 175503 (2014).
[111]C. Coulais, E. Teomy, K. De Reus, Y. Shokef, and M. Van Hecke, Nature **535**, 529 (2016).
[112]S. Janbaz, F. Bobbert, M. Mirzaali, and A. Zadpoor, Mater. Horiz. **6**, 1138 (2019).
[113]A. D. B. Ferreira, P. R. Novoa, and A. T. Marques, Compos. Struct. **151**, 3 (2016).
[114]A. G. Evans, J. Hutchinson, and M. Ashby, Prog. Mater. Sci. **43**, 171 (1998).
[115]C. Li, E. T. Thostenson, and T.-W. Chou, Compos. Sci. Technol. **68**, 1227 (2008).
[116]M. Zhang, S. Fang, A. A. Zakhidov, S. B. Lee, A. E. Aliev, C. D. Williams, K. R. Atkinson, and R. H. Baughman, Science **309**, 1215 (2005).
[117]D. Yu, K. Goh, H. Wang, L. Wei, W. Jiang, Q. Zhang, L. Dai, and Y. Chen, Nat. Nanotechnol. **9**, 555 (2014).
[118]Y. Lin and H. A. Sodano, Compos. Sci. Technol. **68**, 1911 (2008).
[119]M. Lin and F.-K. Chang, Compos. Sci. Technol. **62**, 919 (2002).
[120]Y. Yang, H. Zhang, G. Zhu, S. Lee, Z.-H. Lin, and Z. L. Wang, Acs Nano **7**, 785 (2012).
[121]L. Sun, W. M. Huang, Z. Ding, Y. Zhao, C. C. Wang, H. Purnawali, and C. Tang, Mater. Des. **33**, 577 (2012).
[122]J. M. Jani, M. Leary, A. Subic, and M. A. Gibson, Mater. Des. **56**, 1078 (2014).
[123]M. Behl, M. Y. Razzaq, and A. Lendlein, Adv. Mater. **22**, 3388 (2010).
[124]M. Ashby, A. Evans, L. Gibson, J. Hutchinson, N. Fleck, and H. Wadley, *Cellular Metals, A Design Guide* (Cambridge University, Cambridge, 1998).
[125]Z. Jia, Z. Wang, D. Hwang, and L. Wang, ACS Appl. Energy Mater. **1**, 3 (2018).
[126]P. Vogiatzis, S. Chen, X. Wang, T. Li, and L. Wang, Comput. Aided Des. **83**, 15 (2017).
[127]M. Osanov and J. K. Guest, Annu. Rev. Mater. Res. **46**, 211 (2016).
[128]O. McGee, H. Jiang, F. Qian, Z. Jia, L. Wang, H. Meng, D. Chronopoulos, Y. Chen, and L. Zuo, Addit. Manuf. **30**, 100842 (2019).
[129]J. Oladunni, J. H. Zain, A. Hai, F. Banat, G. Bharath, and E. Alhseinat, Sep. Purif. Technol. **207**, 291 (2018).

[130]Y. Bar-Cohen, J. Spacecr. Rockets **39**, 822 (2002).
[131]P. Panda and B. Sahoo, Ferroelectrics **474**, 128 (2015).
[132]C. Morón, C. Cabrera, A. Morón, A. García, and M. González, Sensors **15**, 28340 (2015).
[133]B. Ghosh and M. W. Urban, Science **323**, 1458 (2009).
[134]L. Christodoulou and J. D. Venables, J. Mater. **55**, 39 (2003).
[135]R. F. Gibson, Compos. Struct. **92**, 2793 (2010).
[136]Y. C. Lai, Y. C. Hsiao, H. M. Wu, and Z. L. Wang, Adv. Sci. **6**, 1801883 (2019).
[137]Z. L. Wang and J. Song, Science **312**, 242 (2006).
[138]H. S. Kim, J. S. Kang, J. S. Park, H. T. Hahn, H. C. Jung, and J. W. Joung, Compos. Sci. Technol. **69**, 1256 (2009).
[139]Y. Kim, H. Yuk, R. Zhao, S. A. Chester, and X. Zhao, Nature **558**, 274 (2018).
[140]B. G. Compton and J. A. Lewis, Adv. Mater. **26**, 5930 (2014).
[141]H. Gao, Int. J. Fract. **138**, 101 (2006).
[142]P. Fratzl and R. Weinkamer, Prog. Mater Sci. **52**, 1263 (2007).
[143]R. Wang and H. S. Gupta, Annu. Rev. Mater. Res. **41**, 41 (2011).
[144]H. Chen, T. Yang, Z. Wu, Z. Deng, Y. Zhu, and L. Li, Acta Biomater. (in press) (2020).
[145]N. Abid, J. W. Pro, and F. Barthelat, J. Mech. Phys. Solids **124**, 350 (2019).
[146]L. Mullen, R. C. Stamp, P. Fox, E. Jones, C. Ngo, and C. J. Sutcliffe, J. Biomed. Mater. Res. B **92**, 178 (2010).
[147]I. Christodoulou and P. Tan, Eng. Fract. Mech. **104**, 140 (2013).
[148]A. Herman, L. Addadi, and S. Weiner, Nature **331**, 546 (1988).
[149]L. Liu, P. Kamm, F. García-Moreno, J. Banhart, and D. Pasini, J. Mech. Phys. Solids **107**, 160 (2017).
[150]X. Cui, Z. Xue, Y. Pei, and D. Fang, Int. J. Solids Struct. **48**, 3453 (2011).
[151]Z. Zhang, Y.-W. Zhang, and H. Gao, Proc. R. Soc. Lond. B **278**, 519 (2011).
[152]D. Li, W. Liao, N. Dai, and Y. M. Xie, Comput. Aided Des. **119**, 102787 (2020).
[153]J. E. Bolander and N. Sukumar, Phys. Rev. B **71**, 094106 (2005).
[154]D. Dimiduk, M. Uchic, and T. Parthasarathy, Acta Mater. **53**, 4065 (2005).
[155]M.-S. Pham, C. Liu, I. Todd, and J. Lertthanasarn, Nature **565**, 305 (2019).
[156]S. P. Reise and N. G. Waller, Ann. Rev. Clin. Psych. **5**, 27 (2009).
[157]X. Zhao, Soft Matter **10**, 672 (2014).
[158]P. Celli, C. McMahan, B. Ramirez, A. Bauhofer, C. Naify, D. Hofmann, B. Audoly, and C. Daraio, Soft Matter **14**, 9744 (2018).
[159]D. Woods, D. Doty, C. Myhrvold, J. Hui, F. Zhou, P. Yin, and E. Winfree, Nature **567**, 366 (2019).
[160]B. O. Okesola and A. Mata, Chem. Soc. Rev. **47**, 3721 (2018).
[161]K. Ariga, M. Nishikawa, T. Mori, J. Takeya, L. K. Shrestha, and J. P. Hill, Sci. Technol. Adv. Mater. **20**, 51 (2019).
[162]Y. Zhang, F. Zhang, Z. Yan, Q. Ma, X. Li, Y. Huang, and J. A. Rogers, Nat. Rev. Mater. **2**, 170149 (2017).
[163]J. Greenhall and B. Raeymaekers, Adv. Mater. Technol. **2**, 1700122 (2017).
[164]J. Li, L. Li, J. Zhou, Z. Zhou, X.-L. Wu, L. Wang, and Q. Yao, Appl. Mater. Today **17**, 206 (2019).
[165]S. Mannan, J. Paul Knox, and S. Basu, R. Soc. Open Sci. **4**, 160412 (2017).
[166]P. Nicholas, E. L. Hernández, and C. Gengnagel, *The Faraday Pavilion: Activating Bending in the Design and Analysis of an Elastic Gridshell* (SimAUD, 2013), p. 1.
[167]Y. Li, Y. Chen, T. Li, S. Cao, and L. Wang, Compos. Struct. **189**, 586–597 (2018).